Chin. J. Astron. Astrophys. Vol. 2 (2002), No. 3, 226–247
( http://www.chjaa.org or http://chjaa.bao.ac.cn )

Chinese Journal of Astronomy and Astrophysics

# History of Star Formation and Chemical Enrichment in the Milky Way Disk

Rui-Xiang Chang[1,2] ⋆, Cheng-Gang Shu[1] and Jin-Liang Hou[1]

[1] Shanghai Astronomical Observatory, Chinese Academy of Sciences, Shanghai 200030
[2] CAS-Peking University Joint Beijing Astronomical Center, Beijing 100871

Received 2001 December 13; accepted 2002 April 5

**Abstract** Based on a physical treatment of the star formation law similar to that given by Efstathiou, we have improved our two-component chemical evolution model for the Milky Way disk. Two gas infall rates are compared, one exponential, one Gaussian. It is shown that the star formation law adopted in this paper depends more strongly on the gas surface density than that in Chang et al. It has large effects on the history of star formation and gas evolution of the whole disk. In the solar neighborhood, the history of chemical evolution and star formation is not sensitive to whether the infall rate is Gaussian or exponential. For the same infall time scale, both forms predict the same behavior for the current properties of the Galactic disk. The model predictions do depend on whether or not the infall time scale varies with the radius, but current available observations cannot decide which case is the more realistic. Our results also show that it would be inadequate to describe the gradient evolution along the Galactic disk by only one word "flatter" or "steeper", as was suggested by Hou et al. and Chiappini et al. We point out that both the absolute value and the evolution of the abundance gradient may be different in the inner and outer regions.

**Key words:** Galaxy: abundance — Galaxy: evolution; formation — Galaxy: star formation

## 1 INTRODUCTION

Models of chemical evolution, which focus on long-term features and average trends of galaxies, have proven to be one of the powerful tools to explore the formation and evolution of galaxies. During the past decades, a large number of such models have been developed, aiming to explore details of the Galactic formation and evolution, either with radial inflows (e.g. Götz & Köppen 1992; Chamcham & Tayler 1994; Tsujimoto et al. 1995; Firmani et al. 1996; Thon & Meusinger 1998; Portinari & Chiosi 2000) or without radial flows (Ferrini et al. 1994; Prantzos

⋆ E-mail: crx@center.shao.ac.cn

& Aubert 1995; Giovagnoli & Tosi 1995; Carigi 1996; Chiapinni et al. 1997, 2001; Allen et al. 1998; Prantzos & Silk 1998); Boissier & Prantzos 1999; Chang et al. 1999; Portinari & Chiosi 1999; Goswami & Prantzos 2000; Hou et al. 2000; Liang et al. 2001). Some promising chemico-dynamical evolutionary models for the Milky Way have also been developed by a few groups (Steinmetz & Müller 1994; Samland et al. 1997; Berczik 1999).

In general, the chemical evolution of the Galaxy has been traditionally studied with semi-analytic and numerical techniques based on a classical set of equations (Pagel 1997). Two important ingredients of the model concern the gas infall rate and the star formation rate (SFR). The later is often determined from the observations. For instance, the form, SFR $\propto \Sigma_g^k$ ($\Sigma_g$ is the gas surface density), was suggested by Kennicutt (1989, 1998) on the basis of the observed average SFR versus gas surface density in spirals. The infall rate is always simply assumed to be either exponential or Gaussian on purely phenomenological grounds in order to account for the "G-dwarf" problem in the solar neighborhood. Indeed, models adopting these forms have been quite successful in reproducing the main features of the Milky Way. We note that comparatively few models without radial flows have attempted to model the Galactic halo (Chiapinni et al. 1997, 2001; Chang et al. 1999; Goswami & Prantzos 2000). In particular, Chiapinni et al. (1997, 2001) and Chang et al. (1999) have suggested a scenario where the Galaxy disk forms as a result of two infall episodes, the thick and the thin disk being formed on two different time scales.

Despite the success, some important differences exist among these various models. The most important one concerns the history of the metal abundance profile: was it steeper or flatter in the past? The former is suggested by the models of Prantzos & Aubert (1995), Mollá et al. (1997), Allen et al. (1998), Boissier & Prantzos (1999), Hou et al. (2000). The latter is supported by those of Tosi (1988) and Chiappini et al. (1997, 2001). However, we shall show in this paper that it would be inadequate to describe the gradient evolution along the Galactic disk simply by "flatter" or "steeper". We argue that the gradient may differ between the inner and outer regions. Its value strongly depends on the chemical composition of the infall material, and it is correlated strictly with the mechanism of Galaxy formation, including the formation of the halo.

In our previous paper (Chang et al. 1999), we have developed a two-component model for the chemical evolution of the Milky Way disk. Both the pre-thin and post-thin scenarios for the formation of the thick disk were considered. In that paper, our main purpose was to explore which scenario (post-thin or pre-thin) is more acceptable by comparing the model predictions and available observed data. It turned out that the post-thin model was more viable.

Here, we present an improved version of the post-thin model, in which a more physical method of treating the law of disk star formation from Efstathiou (2000) is adopted. In this case, the star formation rate is determined by balancing the energy dissipated in collisions between cold gas clouds with that supplied by supernovae in a disk marginally unstable to axisymmetric instabilities (see section 2.3). We also compare two forms of gas infall rate: one is exponential and the other is Gaussian. Our explicit purposes are: (i) to explore the influence of both the new adopted star formation law and two infall rates on the star formation history and gas evolution of the Milky Way disk; (ii) to see the evolution of abundance profiles along the Galactic disk.

In Section 2 we give a brief introduction of the adopted basic model and present detailed descriptions of the assumed infall rate and the new treatment of SFR. Section 3 introduces our adopted observations. Section 4 contains detailed comparisons between our numerical results

and the observational data, and Section 5 presents our conclusions.

## 2 BASIC MODEL

The basic assumptions of the adopted model for the chemical evolution of the Milky Way disk were described in details in Chang et al. (1999). It is assumed that the Galactic disk is sheet-like, which originates and grows only from the infall of cold gas. The disk is considered to be a system of independent rings each 1 kpc wide. Neither radial inflows nor radial outflows are considered. The ring centered at the Galactocentric distance $r_\odot = 8.5$ kpc is labeled as the solar neighborhood.

### 2.1 The Infall Rate

In our previous work (Chang et al. 1999), we have developed a two-component model of the Galactic disk to investigate its chemical evolution. It is assumed that the formation of the thick and thin disks occurs in two main accretion episodes with both infall rates being Gaussian. Both the pre-thin and post-thin scenarios for the formation of the thick disk are considered. For the pre-thin model, the first infall episode forms the thick disk, which originates from a fast dissipative collapse. The second infall episode, which occurs some time later, forms the thin disk component with a time-scale much longer than that of the thick disk. Contrary to the pre-thin model, the post-thin model assumes that the first infall episode forms the thin disk. The thick disk forms later as a result of some actions on or by the thin disk. In the previous paper, we tried to find out which scenario (post-thin or pre-thin) is more acceptable by comparing the model predictions with available observations. It turned out that the post-thin model was more viable. Indeed, this scenario could readily account for the evolution of the solar neighborhood and reproduce quite successfully the main observations (such as the age-metallicity relationship, the metallicity distribution of G dwarfs, the correlation between [O/Fe] and [Fe/H], the present-day local thick disk density). Moreover, the model predictions for the disk as a whole are successful. The adopted best-fit model leads to present-day radial profiles of the SFR, the gas and an oxygen abundance gradient, which are in fair agreement with the observed results.

One of the important ingredients for the model of chemical evolution is the gas infall rate. Current popular models of the disk galaxy formation are semi-analytic models within the framework of hierarchical structure formation theory (White & Rees 1978; White & Frenck 1991; Kauffmann et al. 1993; Mo et al. 1998; Somerville & Primack 1999; Efstathiou 2000), which allow us to model the astrophysical processes involved in a physical way. These models postulate that the formation of a galaxy is mainly regulated by gas cooling, dissipation, star formation, and supernovae feedback. However, for simplicity, chemical evolution models always adopt a simple form of gas infall rate to represent these complicated processes. This choice is acceptable, at least for a first-order investigation. Blitz et al. (1999) has given observational support for this adoption, showing that the Milky Way and M31 are currently accreting substantial amounts of gas ($\sim 1 M_\odot\,\mathrm{yr}^{-1}$) in the form of high velocity clouds of low metallicity. The detection of a massive, low metallicity (0.09 times solar metallicity) cloud falling into the disk of the Milky Way was also reported by Wakker et al. (1999). The authors have given strong arguments for an extragalactic origin for the gas infall.

Therefore, a simple form of gas infall rate can be considered as a simple and alternative method to explore the main features of the gas cooling process at the current stage of knowl-

edge. In fact, it is the obvious advantage of chemical evolution models to explore the intrinsic characteristics of complicate processes which are still unknown, based on simple assumptions (Pagel 1997).

Different forms of gas infall rate have been explored in several models, but not all of them can solve the basic "G-dwarf" problem. Here, we will consider two commonly adopted infall forms in order to explore their differences and influences on the Galactic disk evolution. The free parameters they contain are adjusted so as to give a best fit between the model predictions and observations.

One of the adopted forms is the Gaussian in which the rate of mass accretion (in unit of $M_{\odot}\mathrm{pc}^{-2}\mathrm{Gyr}^{-1}$) in each ring is expressed as

$$f(r,t) = \frac{A(r)}{\sqrt{2\pi}\sigma_t} e^{-(t-\tau_t)^2/2\sigma_t^2} + \frac{B(r)}{\sqrt{2\pi}\sigma_d} e^{-(t-\tau_d)^2/2\sigma_d^2}, \tag{1}$$

where $\tau_t$ and $\tau_d$ (in units of Gyr) are the maximum infall time of the thick and thin disk respectively, $\sigma_t$ and $\sigma_d$ (in units of Gyr) are the corresponding half-widths. It is assumed that $\sigma_t \approx \tau_t$ and $\sigma_d \approx \tau_d$ (Chang et al. 1999). The infall rate $f(r,t)$ is normalized to the present-day local disk density, i.e., $\int_0^{t_g} f(r,t)\,\mathrm{d}t = \Sigma_{\mathrm{tot}}(r,t_g)$, where $\Sigma_{\mathrm{tot}}(r,t_g)$ is the present-day total (star + gas) surface mass density of the ring centered at Galactocentric radius $r$, $t_g$ is the age of the Galactic disk. Assuming that the present-day total masses of the different rings exponentially decrease with increasing Galactocentric distance, both in the thin and thick disk with the same scale-length $r_d$, the form of $A(r)$ and $B(r)$ in the post-thin model can be written respectively as

$$A(r) = \begin{cases} 0 & \text{if } t < t_{\max} \\ \dfrac{\Sigma_{\mathrm{thick}}(r_\odot,t_g)}{\int_{t_{\max}}^{t_g} \frac{e^{-(t-\tau_t)^2/2\sigma_t^2}}{\sqrt{2\pi}\sigma_t}\,\mathrm{d}t} e^{-\frac{r-r_\odot}{r_d}} & \text{if } t_{\max} \le t \le t_g, \end{cases} \tag{2}$$

$$B(r) = \frac{\Sigma_{\mathrm{tot}}(r_\odot,t_g) - \Sigma_{\mathrm{thick}}(r_\odot,t_g)}{\int_0^{t_g} \frac{e^{-(t-\tau_d)^2/2\sigma_d^2}}{\sqrt{2\pi}\sigma_d}\,\mathrm{d}t} e^{-\frac{r-r_\odot}{r_d}}, \tag{3}$$

where $t_{\max}$ represents the epoch at which the formation of the thick disk begins, $\Sigma_{\mathrm{tot}}(r_\odot,t_g)$ is the present-day total surface density in the solar neighborhood, and $\Sigma_{\mathrm{thick}}(r_\odot,t_g)$ is the present-day local surface density of the thick disk.

The other form of the gas infall rate is assumed to be exponential, where the rate of gas infall (in unit of $M_{\odot}\mathrm{pc}^{-2}\mathrm{Gyr}^{-1}$) in each ring is expressed as

$$f'(r,t) = A'(r)e^{-(t/\tau_t')} + B'(r)e^{-(t/\tau_d')}, \tag{4}$$

where $\tau_t'$ and $\tau_d'$ (in units of Gyr) are the infall time scales of the thick and thin disk, respectively. Using the same method described above, the form of $A'(r)$ and $B'(r)$ can be written as

$$A'(r) = \begin{cases} 0 & \text{if } t < t_{\max} \\ \dfrac{\Sigma_{\mathrm{thick}}(r_\odot,t_g)}{\tau_t'(e^{-t_{\max}/\tau_t'} - e^{-t_g/\tau_t'})} e^{-\frac{r-r_\odot}{r_d}} & \text{if } t_{\max} \le t \le t_g, \end{cases} \tag{5}$$

$$B'(r) = \frac{\Sigma_{\mathrm{tot}}(r_\odot,t_g) - \Sigma_{\mathrm{thick}}(r_\odot,t_g)}{\tau_d'(1 - e^{-t_g/\tau_d'})} e^{-\frac{r-r_\odot}{r_d}}. \tag{6}$$

It can be seen that, if $\tau_t$, $\tau_d$ and $t_{max}$ do not vary with radius, Eqs. (1)–(3) guarantee that the disk increases as a whole and is exponential at every step of evolutionary time. If $\tau_d$

increases with radius (which means that the gas cools faster in the inner than the outer disk), then the disk builds up in an "inside-out" scenario, that is, the inner disk forms earlier than the outer disk. The situation is similar for the case of exponential gas infall rate.

To explore the influence of different forms of gas infall on the evolution of Galactic disk, we adopt four models in this paper. See Table 1. These models differ only in the gas infall rate and the infall time scale: all the other ingredients (such as star formation law, stellar initial mass function etc.) are the same.

**Table 1** Four Models Adopted in the Paper

| | gas infall form | $\tau_d$ (or $\tau'_d$) |
|---|---|---|
| Model A | Gaussian | $\tau_d = \tau_\odot$ |
| Model B | Exponential | $\tau'_d = \tau'_\odot$ |
| Model C | Gaussian | $\tau_d = \tau_\odot r/r_\odot$ |
| Model D | Exponential | $\tau'_d = \tau'_\odot r/r_\odot$ |

### 2.2 Initial Mass Function (IMF)

The adopted stellar initial mass function is taken from Kroupa et al. (1993), in which the IMF is described by a three-slope power law, $\phi(m) \propto m^{-(1+x)}$. In the high-mass region the IMF has a relatively steep slope of $x = 1.7$, while it flattens in the low-mass range ($x = 1.2$ for $0.5M_\odot \leq m \leq 1.0M_\odot$ and $x$=0.3 for $m < 0.5M_\odot$). The adopted IMF is normalized to $\int_{0.1}^{100.0} m\phi(m)\,\mathrm{d}m = 1$.

### 2.3 Star Formation Rate (SFR)

Among various ingredients for Galactic evolution studies, the star formation rate is the most important and the least understood. Despite more than 30 years of observational and theoretical work, the Schmidt law still remains popular. However, this kind of treatment is very phenomenological. A more precise description should also be tested in the framework of galaxy formation theory (that is under standard CDM model, Efstathiou 2000). In the present work, we adopt the star formation law similar to that in Efstathiou (2000), to which we refer for a detailed description. The main idea is that the star formation rate is determined by balancing the energy dissipated in collisions between cold gas clouds with that supplied by supernovae in a disk marginally unstable to axisymmetric instabilities. Below we present an overview some of the main features.

The stability criterion for a two-component (stellar and gas) rotating disk can be written as

$$\sigma_g = \frac{\pi G \Sigma_g}{\kappa} g(\alpha, \beta), \tag{7}$$

where $\Sigma_g$ is the gas surface mass density and $\kappa$ is the epicyclic frequency

$$\kappa = 2\omega\Big(1 + \frac{1}{2}\frac{r}{\omega}\frac{\mathrm{d}\omega}{\mathrm{d}r}\Big)^{1/2}, \tag{8}$$

in which $\omega$ is the circular frequency. The quantities $\alpha$ and $\beta$ are related to the vertical velocity dispersion $\sigma_*^2$ and surface mass density $\Sigma_*$ of the star to those of the gas cloud

$$\sigma_* = \alpha\sigma_g, \qquad \Sigma_* = \beta\Sigma_g. \tag{9}$$

Here we assume $\alpha = 5$ (Efstathiou 2000). Equation (7) is identical to the Goldreich-Lyden-Bell criterion except for the factor $g(\alpha, \beta)$. We refer to Efstathiou (2000) and Jog & Solomon (1984) for details of the calculation of $g(\alpha, \beta)$.

For the IMF adopted in this paper, one supernova is formed for every $250 M_\odot$ of star formation assuming that massive stars ($m > 9 M_\odot$) explode as supernovae and release $10^{51} E_{51}$ erg in kinetic energy. Therefore, the energy injection rate per unit surface area (in units of erg $\mathrm{s}^{-1}\mathrm{pc}^{-2}$) can be expressed as

$$\dot{E}^{\Omega}_{\mathrm{SN}} = 1.3 \times 10^{32} E_{51} \psi, \tag{10}$$

where $\psi$ is the star formation rate in $M_\odot \mathrm{pc}^{-2}\mathrm{Gyr}^{-1}$.

On the other hand, cold clouds lose energy through inelastic collisions. The rate of energy loss per unit surface area (in units of erg $\mathrm{s}^{-1}\mathrm{pc}^{-2}$) is given by

$$\dot{E}^{\Omega}_{\mathrm{coll}} = 5.0 \times 10^{29} \Big(1 + \frac{\beta}{\alpha}\Big) \Sigma^3_{g5} \sigma_{g5}, \tag{11}$$

where $\Sigma_{g5}$ is the gas surface mass density in units of $5 M_\odot \mathrm{pc}^{-2}$ and $\sigma_{g5}$ is the cloud velocity dispersion in units of $5\,\mathrm{km\ s}^{-1}$.

Assuming that the energy lost in cloud collisions is balanced by a constant fraction $\epsilon_c$ of the energy input from supernovae $\epsilon_c \dot{E}^{\Omega}_{\mathrm{SN}} = \dot{E}^{\Omega}_{\mathrm{coll}}$, then, the star formation rate (in units of $M_\odot \mathrm{pc}^{-2}\mathrm{Gyr}^{-1}$) is given by

$$\psi(r, t) = \frac{3.8 \times 10^{-3} (1 + \beta/\alpha) \Sigma^3_{g5} \sigma_{g5}}{\epsilon_c E_{51}}. \tag{12}$$

In this model $\epsilon_c$ is a free parameter.

To obtain the epicyclic frequency $\kappa$, the circular speed of both the halo and the disk should be known. It is assumed that the dark halo can be described by the Navarro, Frenk & White (1996) profile. The circular speed corresponding to this profile is

$$v^2_H(r) = v^2_v \frac{1}{x} \frac{[\ln(1 + cx) - cx/(1 + cx)]}{[\ln(1 + c) - c/(1 + c)]}, \qquad v^2_v \equiv \frac{G M_v}{r_v}, \tag{13}$$

where $x \equiv r/r_v$, $r_v$ is the virial radius at which the halo has a mean overdensity of 200 with respect to the background, $M_v$ the mass of the halo within the virial radius and $c$ a concentration parameter.

We assume that the disk surface mass density distribution at the current time is described by an exponential

$$\Sigma_{\mathrm{tot}}(r, t_g) = \Sigma_0 e^{-r/r_d}, \qquad M_{\mathrm{D}} \equiv 2\pi \Sigma_0 r^2_d, \tag{14}$$

where $\Sigma_{\mathrm{tot}}(r, t_g)$ is the total (star + gas) surface mass density of the ring centered at Galactocentric radius $r$, $M_{\mathrm{D}}$ the total disk mass and $r_d$ the disk scale length. The rotation curve of a cold exponential disk is given by Freeman (1970)

$$v^2_{\mathrm{D}}(r) = 2 v^2_c y^2 [I_0(y) K_0(y) - I_1(y) K_1(y)], \tag{15}$$

where $y \equiv \frac{1}{2} \frac{r}{r_d}$ and $v^2_c \equiv \frac{G M_{\mathrm{D}}}{r_d}$. The ratio of disk scale length to virial radius of the halo is defined as the collapse factor, and it is assumed $\frac{r_v}{r_d} \equiv f_{\mathrm{coll}} = 50$ (Efstathiou 2000).

In summary, the disk of stars and gas is constrained to satisfy the stability criterion of Equation (7), which fixes the cloud velocity dispersion $\sigma_g$. The star formation rate is regulated by the energy balance between cloud collisions and supernovae explosions. Accordingly, the final form of the star formation rate is derived by inserting Equation (7) into Equation (12).

### 2.4 Stellar Ejecta and Nucleosynthesis

We assume that, except for Type Ia supernovae (SNIa), any star evolves as a single star even if it is a member of a binary system. It is also assumed that every single star ejects its envelope just after leaving the main sequence. All massive stars ($m > 9M_{\odot}$) explode as type II supernovae (SNII), leaving behind a neutron star of mass $m_R = 1.4M_{\odot}$. The final stage of the intermediate /low mass star ($M \leq 9M_{\odot}$) is a white dwarf. SNIa are thought to originate from carbon deflagration in C-O white dwarfs in binary systems. The treatment of the contribution of SNIa is the same as that of Matteucci & Greggio (1986).

We concentrate in this paper on the evolution of the abundance of iron and oxygen, although the initial metallicity has a large effect on stellar yields, this effect can be ignored for iron and oxygen (see figure 1 of Goswami & Prantzos 2000). So the yields obtained from the solar metallicity SNII and SNIa model are adopted in this paper (Woosley & Weaver 1995; Woosley 1997).

## 3 OBSERVATIONAL CONSTRAINT

A successful model of the chemical evolution of the Galactic disk should reproduce the main observational features of both the solar neighborhood and the whole disk. The main observations considered here are: (1) the metallicity distribution of long-lived G-type stars in the solar neighborhood; (2) the current surface densities of gas, star and SFR in the solar neighborhood; (3) the age-metallicity relation (AMR); (4) the [O/Fe] vs. [Fe/H] relation, interpreted in terms of a delayed appearance of SNIa, which produces most of the Galactic iron; (5) the radial abundance profile, obtained from nebulae and early young stars; (6) the radial profile for the gas surface density; and (7) the variation of the Star Formation Rate (SFR) along the Galactic disk radius.

We have selected two observational constraints, the current gas surface density and the G-dwarf metallicity distribution function in the solar neighborhood to constraint the free parameters in the model. The other observations are used for comparison with the model predictions.

**Table 2** Input Parameters

| Parameter | Values | References |
|---|---|---|
| $r_d$ (kpc) | 2.7 | Robin et al. (1996) |
| $\Sigma_{\rm tot}(r_{\odot}, t_g)$ $(M_{\odot}\cdot{\rm pc}^{-2})$ | 55.0 | Rana (1991) |
| $\Sigma_{\rm thick}(r_{\odot}, t_g)$ $(M_{\odot}\cdot{\rm pc}^{-2})$ | 10.0 | Chang et al. (1999) |
| $t_{\rm max}$ (Gyr) | 1.0 | Chang et al. (1999) |
| $\tau_t$ or $\tau_t'$ (Gyr) | 1.0 | Chang et al. (1999) |
| $v_v/v_c$ | 0.45 | Efstathiou (2000) |
| c | 10 | Efstathiou (2000) |
| $\alpha$ | 5 | Efstathiou (2000) |
| $t_g$ (Gyr) | 13 | Rana (1991) |
| $\tau_d$ or $\tau_d'$ | free parameter | |
| $\epsilon_c$ | free parameter | |

## 4 NUMERICAL RESULTS AND DISCUSSION

We numerically solve the classical set of equations of galactic chemical evolution (Chang et al. 1999). The instantaneous-recycling approximation (IRA) is relaxed, but instantaneous mixing of the gas with the stellar ejecta in a given ring is assumed, i.e., the gas is characterized by a unique composition at each epoch of time. The initial condition is that the disk surface mass density is zero. Then, the cold disk builds up gradually at a rate given by Equation (1) or (4). The star formation rate is regulated by Equations (7) and (12). It should be emphasized that the epicyclic frequency $\kappa$ varies as the mass of the disk increases with the evolutionary time. The circular speed of the disk component (Equation (15)) is simply re-scaled by the square root of the disk mass at each time step (note: $v_c^2 \equiv \frac{GM_{\rm D}}{r_d}$) .

### 4.1 The Solar Neighborhood

Table 2 lists the input parameters in our model. There are two free parameters: $\tau_d$ in Equation (1) (or $\tau_d'$ in Equation 4) and the efficiency factor $\epsilon_c$ in Equation (12). These two parameters are chosen to reproduce the observed properties of the solar neighborhood, namely the G-dwarf metallicity distribution function and the present-day gas surface density, which is: $\Sigma_g(r_\odot, t_g) = 10.0 M_\odot {\rm pc}^{-2}$ (Scoville & Sanders 1987; Prantzos & Aubert 1995; Sackett 1997).

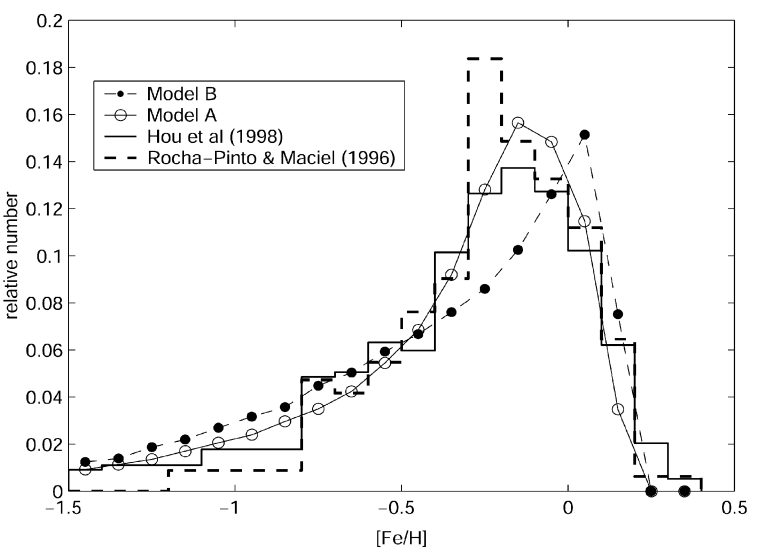


Fig. 1 Results of Model A (solid curve with open circles) and Model B (dash curve with filled circles) for the G-dwarf metallicity distribution in the solar neighborhood. The observed data are taken from Hou et al. (1998) (solid histogram) and Rocha-Pinto & Maciel (1996) (dash histogram).

For the solar neighborhood, Model A is identical with Model C and Model B with Model D. So we only need to compare the predictions of Model A and Model B. We perform model calculations for a broad range of free parameters ($\tau_d$ or $\tau_d'$, $\epsilon_c$). It turned out that Model A with $\tau_d = 3.8\,{\rm Gyr}$, $\epsilon_c = 0.03$ and Model B with $\tau_d' = 3.8\,{\rm Gyr}$, $\epsilon_c = 0.035$ gave a better fit to the value

$\Sigma_g(r_\odot, t_g) = 10.0 M_\odot \mathrm{pc}^{-2}$ and the G-dwarf metallicity distribution function. The comparisons are given in Figure 1 for the G-dwarf metallicity distribution and Figure 2 (upper panel) for the present day gas surface density. These two set of parameters are adopted for the corresponding models throughout this paper.

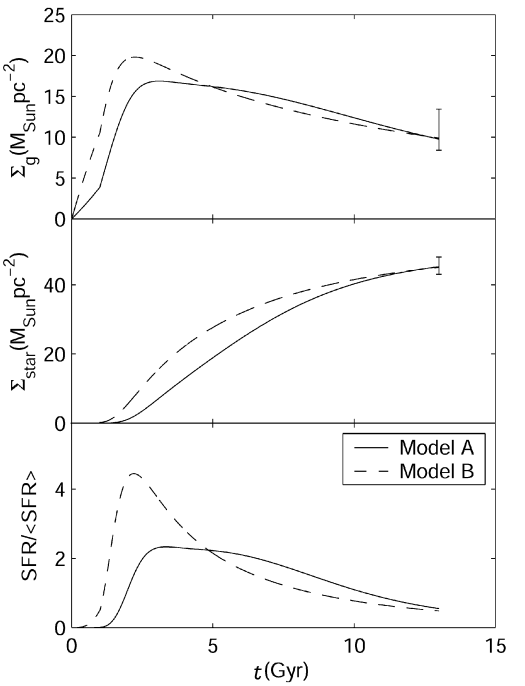


Fig. 2 Time evolution of various quantities in the solar neighborhood predicted by Model A (solid lines) and Model B (dash lines). The error bars indicate observed ranges, which are taken from Boissier & Prantzos (1999).

Figure 1 compares the predicted G-dwarf metallicity distribution with the observational data from Hou et al. (1998) (solid histogram) and Rocha-Pinto & Maciel (1996) (dash histogram). Using a method similar to that of Rocha-Pinto & Maciel (1996), Hou et al. (1998) recalculated the metallicity distribution without the chemical criterion that Rocha-Pinto & Maciel (1996) have used to exclude the halo stars. The resulted distribution which Hou et al. (1998) derived is similar to the final distribution of Rocha-Pinto & Maciel (1996), except for the metal-poor tail. Figure 1 shows that a reasonable agreement between the predictions and observations is reached for both models, but the low metallicity tail is higher in the models than in the data. It can also be seen that the model A gives a better agreement with the observations, and that Model B predicts a sharp cutoff of metal-rich stars. The small difference between Figure 1 and the figure in Chang et al. (1999) results from the different treatment of the star formation law. However, as we will see in Section 4.4, the effect of the SFR is mainly on the past evolution of the disk.

Recently, Haywood (2001) presented a revised metallicity distribution of dwarfs in the solar neighborhood. This distribution differs greatly from that of Rocha-Pinto & Maciel (1996) and

Hou et al. (1998): it is centered at [Fe/H] $\sim$ 0, not [–0.3, –0.1]. To accommodate this new distribution, the infall time scale in our models must be increased since a larger time scale corresponds to a higher peak and may push the peak into a higher metallicity tail. Moreover, the fraction of Type Ia supernovae must be increased in order to reproduce a larger number of metal rich stars. Nevertheless, this would result in a higher ratio of SNIa to SNII, which contradicts the observations. In short, which distribution represents better the real situation still needs further exploration.

Figure 2 shows the time evolution of gas, star and star formation rate in the solar neighborhood predicted by Model A (solid lines) and Model B (dash lines). The star formation history (bottom panel) is represented by the ratio of SFR at evolutionary time $t$ to the average SFR during the whole lifetime, as suggested by Scalo (1986). It can be seen that the star formation rate is almost zero at early times when the gas surface density is low. It suggests that the disk stability criterion has a large effect on the star formation history of the Galactic disk. We will discuss these effects further in Section 4.4.

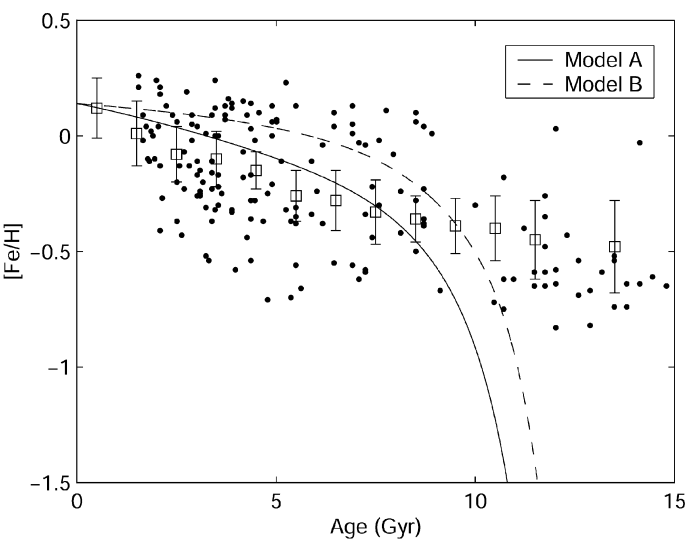


Fig. 3 The age-metallicity relation in the solar neighborhood predicted by Model A (solid lines) and Model B (dash lines). Observational data are taken from Rocha-Pinto et al. (2000b) (squares with error bar) and Edvardssen et al. (1993) (points).

Figure 2 also shows that Model A and Model B predict different histories of star formation in the solar neighborhood. It is important to find out if the observations can point to which model is better. Based on a chromospheric age distribution of 552 late-type dwarfs, Rocha-Pinto et al. (2000a) derived a star formation history in the solar neighborhood. Evidence for at least three epochs of enhanced star formation in the Galaxy disk was found. It should be emphasized that these authors paid much more attention to the variation of the SFR than to the overall average picture. Therefore, it is difficult to compare our results with theirs since a smooth gas infall rate is adopted in our model, which can only predict a smooth star formation history. In a forthcoming paper, we will discuss whether an intermittent gas infall rate can or cannot reproduce such an irregular star formation history.

After calibrating the free parameters from the G-dwarf metallicity distribution and the current gas surface density in the solar neighborhood, we now present the model results for the age-metallicity relation in Figure 3 (solid lines for Model A, dashed lines for Model B). The observational data are taken from Rocha-Pinto et al. (2000b) (squares with error bar) and Edvardssen et al. (1993) (points). The overall trends of the model predictions are consistent with those of the observations, but the present model cannot reproduce the large observed scatters. Our results suggest that orbital diffusion in a homogeneous galaxy is not sufficient to explain the scatter because our model prediction for the present abundance gradient near the solar circle is small (see Figure 8). Moreover, if orbital diffusion is the main producer of the scatter, the scatter should increase with age since the abundance gradient gets steeper in time (see Figure 10).

Our model results for the [O/Fe] vs. [Fe/H] relation are shown in Figure 4. The recent observed data are also given. As expected, both models A and B could reflect well the observed behavior, the steady decline from [O/Fe] $\sim 0.5$ in the [Fe/H] $< -1$ range (that is, during the halo phase) to [O/Fe] $\sim$ solar at [Fe/H] $\sim 0$. This is usually attributed to a delayed ($\sim 1$ Gyr) appearance of SNIa. Note that the open diamonds are from observations of Israelian et al. (1998), which show a continuous increase of [O/Fe] in the low metallicity. There are indeed alternative explanations for this (Goswami & Prantzos 2000; Qian & Wasserburg 2001), but it is not yet settled observationally: the data in the figure are for illustration only.

In summary, we see that adopting different infall laws does not produce any significant effect on the chemical properties of the solar neighborhood. The star formation rate is almost zero at early time when the gas surface density is low. This indicates that the disk stability criterion has large effects on both the star formation history and the abundance profile along the Galactic disk.

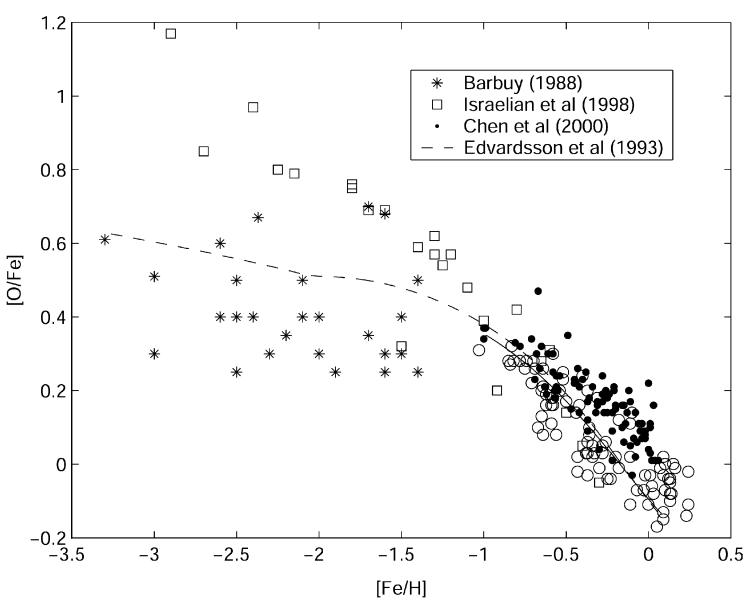


Fig. 4 Comparisons between the observed correlation between [O/Fe] and [Fe/H] and our calculated results of Model A (solid line) and Model B (dash line). The observed data are taken from Barbuy (1988) (asterisks), Israelian et al. (1998) (diamonds), Chen et al. (2000) (points) and Edvardsson et al. (1993).

### 4.2 Radial Profile of Gas Density and Star Formation Rate

Now we turn to the radial profiles of the gas density and star formation process. A successful model should not only reproduce the observed data in the solar neighborhood, but should also agree with the main profiles for the whole disk.

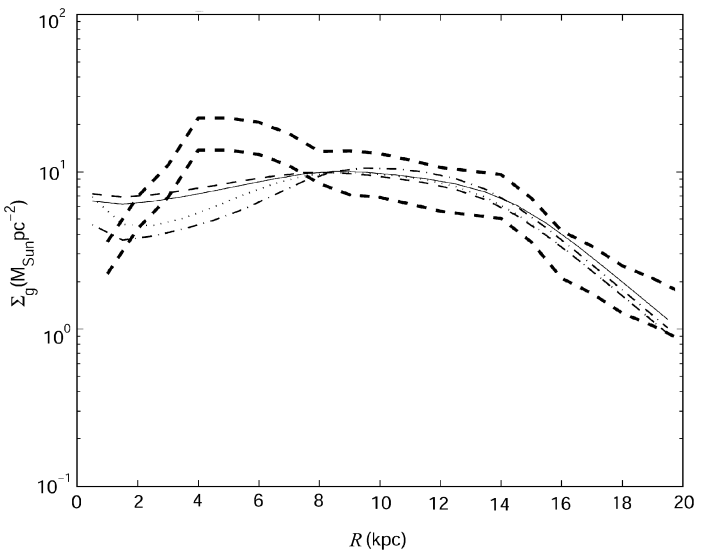


Fig. 5 Comparisons between observations of the present-day radial profile of gas surface density and the predictions of Model A (solid line), Model B (dash line), Model C (dot-dash line) and Model D (dot line). Two thick dash lines mark the observed range for the gas surface density taken from Dame (1993).

Since there is essentially no constraint on the past history of the Milky Way disk (abundance gradient from Planetary Nebula and open clusters might be a tracer, see Hou et al. 2000; however, see discussion in Section 4.3), there is much more freedom in its modeling than for the solar vicinity. Of the set of observational data, the radial distribution of gas surface density is the most difficult to reproduce by our models. Our four models (A to D) can fit quite well the observed data in the outer regions ($r > r_{\odot}$), but we obtain a rather broad distribution around 4 to 6 kpc, while the observed data show a peak there, as can be seen in Figure 5. The chemical evolution model focuses on long-term phenomena and average trends of galaxies and does not consider the influence of dynamical evolution. So it is very difficult for the model to fully reproduce the observed gaseous profile in the inner Galaxy since other factors may have shaped the profile there, e.g., the presence of a bar that induced radial inflows and enhanced the local SFR.

However, models A to D can all reproduce reasonably well the radial profile of the current star formation rate, as shown in Figure 6. It can be seen from Figures 5 and 6 that there are no real differences between predictions of Model A and Model B, or between Model C and Model D. This suggests that, if the adopted infall time scale is similar, then both the Gaussian and the exponential form of infall rate will yield a similar behavior for the current profile of the whole disk, although they predict very different gas evolution histories (see Figure 2).

Significant difference exists between the predictions of Model A and Model C for the inner region of the disk ($r < r_{\odot}$). Since a model of shorter infall time scale corresponds to a faster process of star formation and gas consumption, Model C predicts a deeper inner hole in the radial gas profile (Figure 5) and a weaker variation of star formation rate across the disk (Figure 6) than does Model A. There is a similar difference in the behaviors of Models B and D.

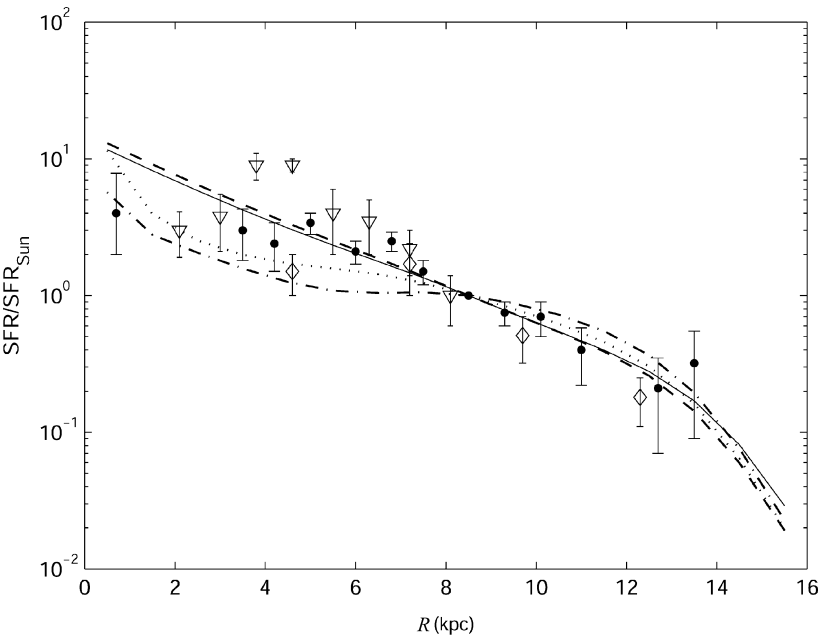


Fig. 6 Comparisons between observations for the present-day radial profile of star formation rate and the predictions of Model A (solid line), Model B (dash line), Model C (dot-dash line) and Model D (dot line). The observed data with error bars are taken from Gusten & Merger (1983) (triangles), Lyne et al. (1983) (dots) and Guibert et al. (1978) (circles), normalized to the star formation rate in the solar neighborhood.

Since Model A and Model C represent different scenarios of disk formation, we display in Figure 7 the predicted radial profiles of Model A (two left panels) and Model C (two right panels) for both the total (gas + star) density and the gas-only density at four different evolutionary times $t = 3$, 6, 9 and 13 Gyr. It can be seen that the radial dependence of infall time scale has great influences on the evolution of the surface densities. However, as we see from Figures 5, 6 and 8 (in Section 4.3), it is difficult to conclude, from the current observed radial profiles, which of the two cases, dependence or independence of the time scale on the radius, is the more realistic one.

According to the adopted infall form, if $\tau_d$ does not vary with radius, the disk keeps the exponential form with scale length $r_d = 2.7$ kpc at each epoch of evolutionary time. The mass density at different radius will increase as a whole with the same rate. However, Model C predicts that the inner disk builds up faster than does the outer disk because of the assumption that the infall time scale increases with the galactocentric distance. The total mass density of the disk can still be roughly expressed as exponential, but its scale length is no longer a constant and increases with time, which is consistent with results of some analytical models

of disk galaxy formation (Mo et al. 1998). However, for the sake of simplicity, in the model calculations, a constant scale length is adopted. This is inconsistent with the real situation but is acceptable as a first order approximation.

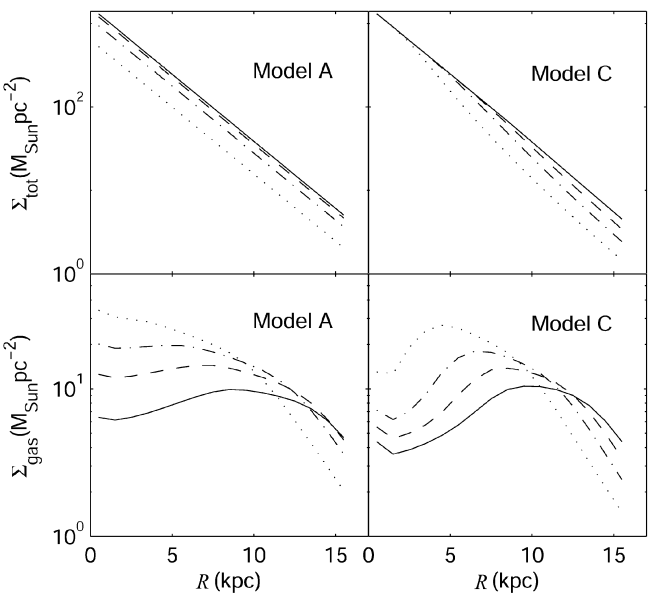


Fig. 7 Results of Model A and Model C for the radial profile of total (gas + star) and gas density at different evolutionary times $t = 3$ Gyr (dotted lines), 6 Gyr (dot-dash lines), 9 Gyr (dash lines) and 13 Gyr (solid lines).

### 4.3 Abundance Profile along the Galactic Disk

Abundance gradients constitute one of the most important constraints for models of the evolution of the Milky Way disk. The existence of such gradients is now well established and offers an opportunity to test theories of disk evolution and stellar nucleosyhthesis. Among different elements, oxygen is one of the best tracers in determining the radial abundance profile along the Milky Way disk. An average gradient of $\mathrm{d}\log(\mathrm{O/H})/\mathrm{d}R \sim -0.07$ dex kpc$^{-1}$ is obtained in the Milky Way disk through radio and optical observations of HII regions, early-type B stars and planetary nebulae (see Hou et al. 2000; Chiappini et al. 2001 for a compilations of the abundance gradients). When we plot all the available data, a significant scatter (up to 1.0 dex) exists at a given radius. Observed abundance data for the outermost part of the disk are still rare. However, after a consistent analysis of their own and previous data on HII regions, Deharveng et al. (2000) concluded that the gradient is about $-0.04$ dex kpc$^{-1}$, $\sim 40$ % smaller than was generally thought. Recently, Smartt et al. (2000) found that the oxygen abundance of B stars in the inner Galaxy is compatible to that in the solar neighborhood. That means a zero gradient for the inner disk.

Our predictions for the current abundance gradients are plotted in Figure 8. Four cases (A, B, C and D) are presented. The observed data are taken from different references, as indicated in the caption of Figure 8. From Fig. 8 we can find: (i) The four models are indistinguishable

in the inner region, while small differences exist in the outer region. This indicates that the resulted abundance distribution is not sensitive to details of the gas infall process after the star formation and chemical enrichment have reached a certain level. However, the gas infall rate has a large influence on the early stage of the disk evolution or on the properties of the outer region of the disk when (or where) no significant star formation occurs. (ii) There is no gradient in the inner region, consistent with the recent data of Smartt et al. (2000). This is due to the fact that the metal abundance is diluted by the numerous low-mass, long-lived stars of the first stellar generation. The ejection rate of that material at late times is greater than the metal production rate since most of the gas in the inner disk has been consumed at that time. (iii) A steep gradient exists in the outer part of the disk. It seems inconsistent with the current available data, which show a flatter oxygen gradient in the outer part of the disk. The reason is that in our simulated "inside-out" infall model, there is always less gas density in the outer region where no significant star formation takes place, and hence, less metal is produced.

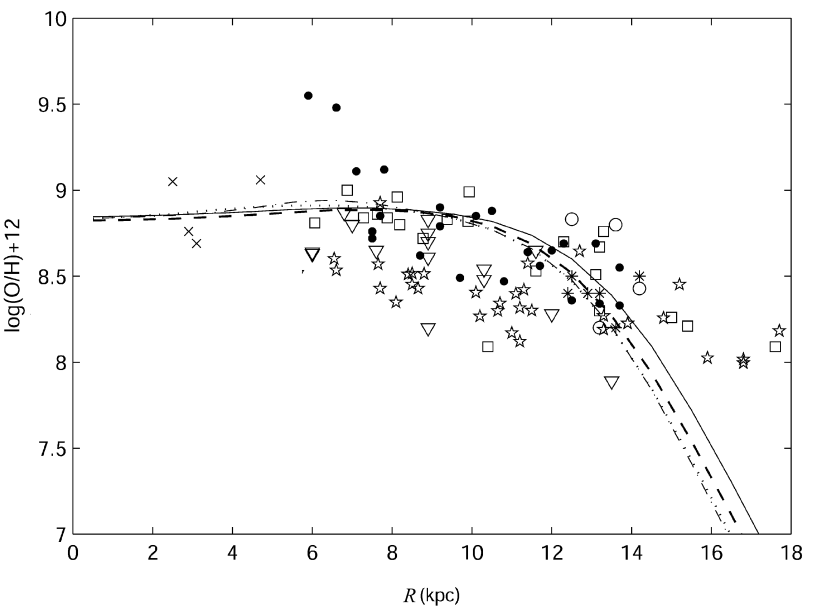


Fig. 8 Radial distribution of the oxygen abundance at the present time predicted by Model A (solid line), Model B (dash line), Model C (dot-dash line) and Model D (dot line). The observed data of HII regions are from Shaver et al. (1983) (points), Fich & Silkey (1991) (open circles), Vilchez & Esteban (1996) (asterisks) and Deharveng et al. (2000) (pentagrams). The observations of early B-type main-squence stars are taken from Smartt et al. (1997) (open squares), Gummersbach et al. (1998) (triangles) and Smartt et al. (2000) (crosses).

The problem could partially be solved by adopting a PIE (Prompt Initial Enrichment) model which assumes that the infalling gas from the halo has been already enriched. In this model, we assume that the infalling gas has metallicity [O/H]$= -1.0$. The other ingredients are the same as in Model A. The result is plotted in Figure 9. Due to the fact that star formation rate is very low in the outer disk, the solid line in Figure 9 flattens slowly with increasing radius, which seems compatible with the observations. Therefore, although the pre-enriched or

primordial infalling gas has little effects on the chemical evolution of the solar neighborhood, it does influence the radial distribution of elemental abundance, especially the distribution in the outer disk.

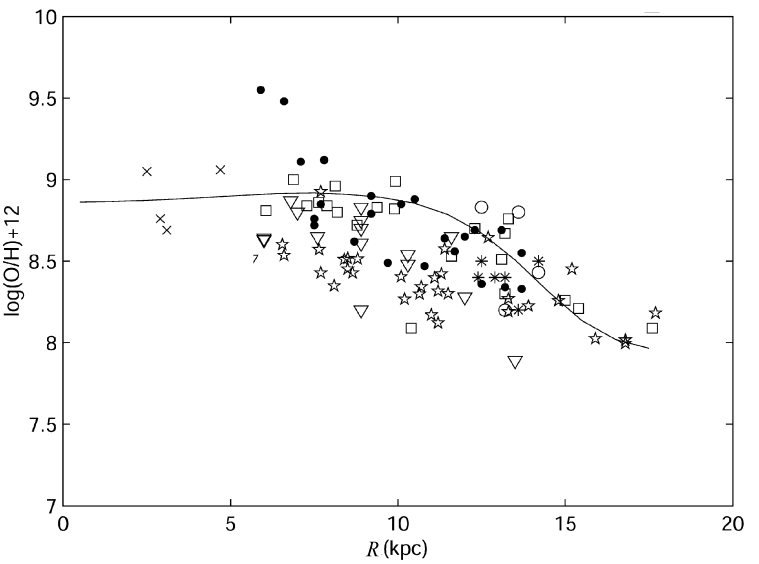


Fig. 9 Comparison of PIE model predictions with observations for the oxygen gradient. Observational data are the same as that of Figure 8.

It should be pointed out that the chemico-dynamical model for the Milky Way (Samland et al. 1997) predicted an oxygen abundance gradient that flattens considerably in the outer disk, which agrees with Figure 9. Observations of Vilchez & Esteban (1996) and Maciel & Quireza (1999) also suggested such a flattening although Deharveng et al. (2000) argued that there is no convincing observational evidence for this up to now.

Although most chemical evolution models could successfully predict the current radial abundance profile, there still exists important difference concerning the history of the abundance gradient: Was it steeper or flatter in the past? The former is suggested by the models of Prantzos & Aubert (1995), Molla et al. (1997), Allen et al. (1998), Boissier & Prantzos et al. (1999), Hou et al. (2000), while the latter is supported by the models of Tosi (1988), Chiappini et al. (1997, 2001). The situation is not settled observationally either (see discussion in Hou et al. 2000). We have computed, for two cases, the evolution of the oxygen abundance gradient, see Figure 10. The upper panel is for Model A, and the lower panel is the PIE model. Two points can be made: (i) In Model A, the oxygen abundance gradient is steeper at early stage of the disk formation and it flattens as a stellar disk is built up gradually. This result agrees with those models that predict a flattening in time. It is also a reasonable result of those models that form the disk "inside-out" from the primordial infalling gas. (ii) A different behavior appears in the PIE model, which shows similar trends to those in Chiappini et al. (2001). Here, the abundance in the outer disk is heavily dependent on the chemical composition of the infalling gas. Since our adopted SFR is related to the disk instability (hence to the gas surface density), the effect of such a treatment is to maintain an almost constant metallicity at large radius

where gas is always relatively low and star formation rate is also low. This is nearly identical to the treatment of Chiapinni et al. (2001) who adopted a threshold gas density for the SFR.

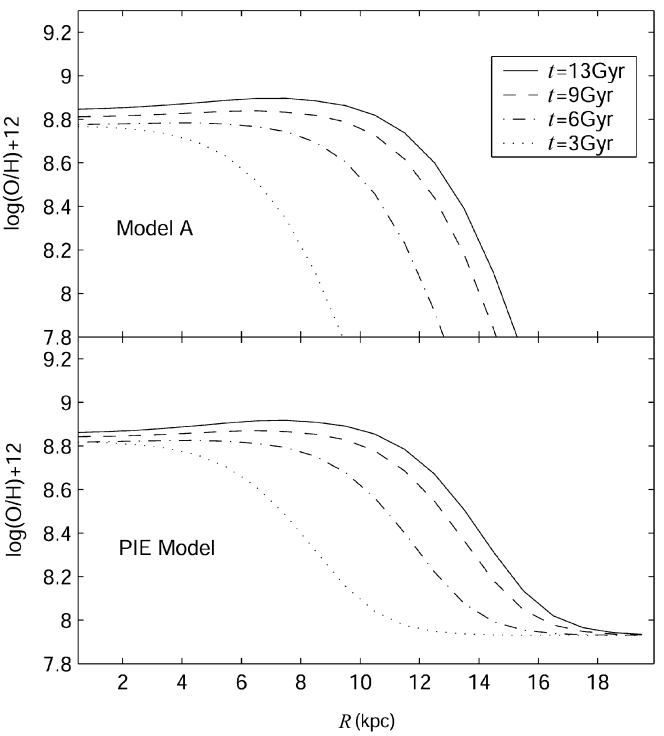


Fig. 10 Evolution of radial distribution of oxygen abundance predicted by Model A (upper panel) and the PIE model (lower panel). Different lines refer to different evolutionary times.

In summary, it is probable that the gradient along the Galactic disk cannot be described by a single value, that the time evolution cannot be described by only a single word, "steeper" or "flatter". The value of a single linear gradient strongly depends on how it is calculated. It is true that a finite gradient exists since the abundance is low in the outer region and high in the inner disk. However, the situation could be different between the inner and outer disk as can be seen in Figure 10. For the inner region (galactocentric distance less than 10 kpc, say), both models (that is, model with primordial infalling gas and the PIE model) predict a gradient flattening with time. For the outer region, Model A predicts no significant time variation of the gradient, at a value greater than that for the inner disk, whereas the PIE model predicts a (possibly) steepening tendency of the gradient. There are some observational hints for different gradients for both the inner and outer disks. Simpson et al. (1995) suggested a two-step distribution of the current oxygen abundance along the Galactic disk based on their infrared line observations of HII regions. From a sample of open clusters, Twarog et al. (1997) also proposed a two-step iron abundance distribution on the Milky Way disk with transition around 10 kpc. Theoretically, the gradient evolution not only depends on the adopted forms of SFR and infall rate, but is also heavily affected by the chemical composition of the infalling gas.

### 4.4 Role of Different Star Formation Laws

Star formation rate (SFR) is one of the most important ingredients of Galactic chemical evolution model. Most of models adopt some empirical forms of SFR based on observations (e.g. Kennicutt 1998). We now compare the results of Model A with those of the post-thin model in Chang et al. (1999) which uses the following SFR:

$$\psi'(r,t) = \nu\Sigma_g^{1.5}(r,t)/r, \tag{16}$$

where $\nu$ is constrained to reproduce the current gas surface density of the solar neighborhood. We denote this model as Model E. It should be noticed that all the other ingredients of Model E are the same as in Model A.

A comparison for the solar neighborhood is given in Figure 11, where we show the time evolution of the gas density (upper panel) and the SFR (lower panel) for Model A (solid line) and Model E (dash line). It can be seen that, at early time ($t < 1.5\,\mathrm{Gyr}$), Model A predicts a smaller SFR than does Model E, although the gas surface densities are almost same. Then, in Model A, the SFR increases rapidly and reaches a peak value earlier than in Model E. This means that Model A predicts a faster star formation and gas consumption process in the solar neighborhood. As time goes on, the SFR in Model A decreases faster than in Model E due to a more rapid gas consumption, but both models give final values that are compatible with the observations. Therefore, the adopted SFR in this paper depends more strongly on the gas surface density than in Equation (16).

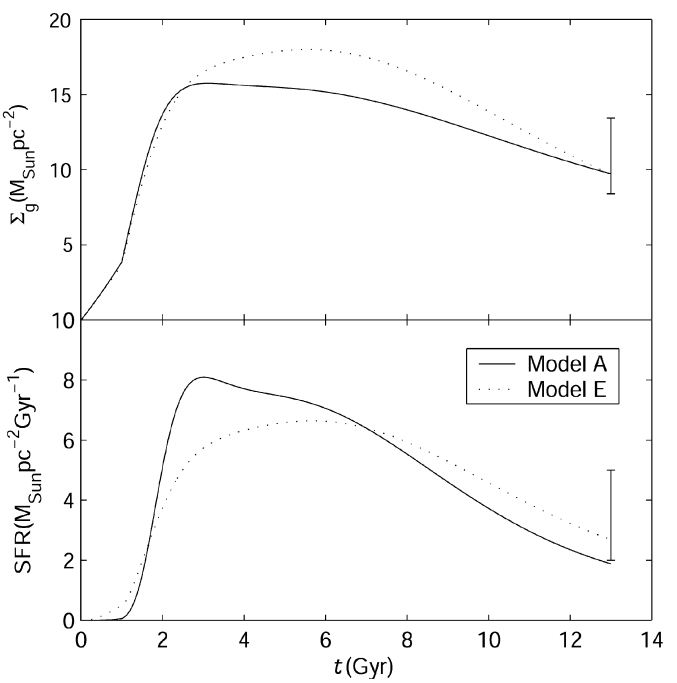


Fig. 11 Predictions of Model A (solid lines) and Model E (dash lines) for the time evolution of gas density and star formation rate in the solar neighborhood.

The predicted radial profiles for the two models are displayed in Figure 12: upper panel for the current gas surface density, middle panel for the SFR, lower panel for the oxygen abundance. From Fig. 12 we gather that (i) The predicted current gas surface density by Model A is lower in the inner region and higher in the outer region compared to Model E. This is because the star formation law adopted in Model A depends more strongly on the gas density. It predicts that gas consumption is faster in the inner than in the outer region, consistent with the results given in Figure 12. (ii) The radial profiles of SFR are similar for most regions of the disk. This is partly due to the fact that the star formation rate is normalized to the solar neighborhood. However, in the outer edge of the disk ($r > 14\,\mathrm{kpc}$), the dash line begins to become higher than the solid line, especially for the metallicity profile (see lower panel of Figure 12). This is because the star formation law adopted in Model E depends more weakly on the gas surface density. It predicts a higher star formation rate than Model A when the gas surface density is low.

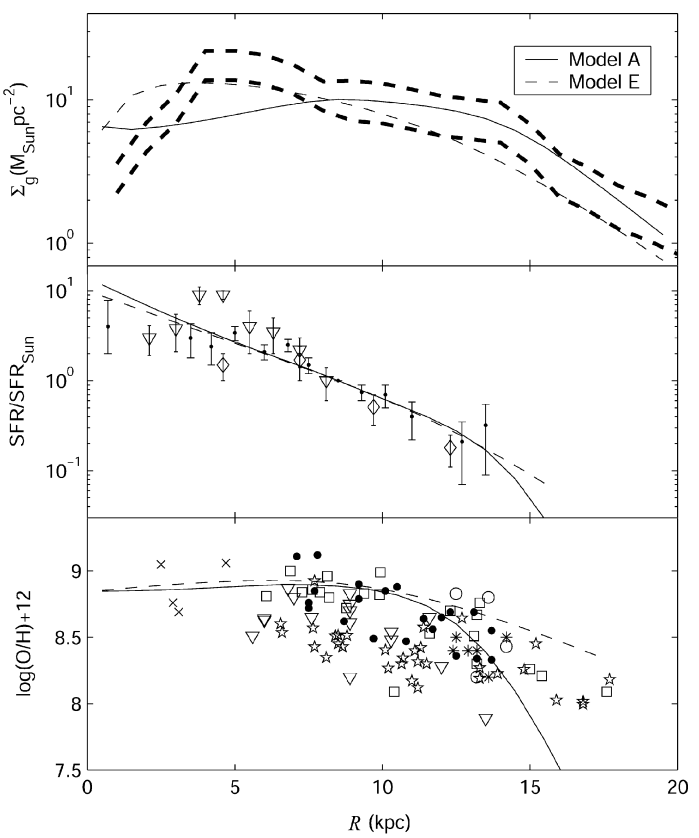


Fig. 12 Predicted present-day radial profiles of gas surface density (upper panel), star formation rate (middle panel) and abundance (lower panel). Models A and E are plotted with solid lines and dash lines, respectively. Observed data are the same as in Figures 5, 6 and 8.

An important fact is that Model A predicts a very low star formation rate in the outer edge of the disk. It suggests that the star formation law presented by Efstathiou (2000) can predict that the stellar disk is truncated at about the Holmberg radius ($r/r_d \approx 5$), which is in rough agreement with the observations. No arbitrary threshold for star formation is needed.

In summary, the star formation law adopted in this paper depends more strongly on the gas surface density than that in Chang et al. (1999). It has large effects on star formation, gas evolution and metallicity of the disk, especially for the outer region of the disk.

## 5 SUMMARY

Based on a new treatment of SFR and two forms of infall laws, we have improved our previous two-component chemical evolution model for the Milky Way disk. The gas infall rate is assumed to be a simple function of Galactocentric radius and evolutionary time. To explore the influence of different gas infall forms on the evolution of Galactic disk (gas density, SFR, metallicity profile and so on), we use four different models. Comparisons between the model results and observations for both the solar neighborhood and the whole disk are presented. We also discuss the influences of different star formation laws on Galactic gas evolution. The main results can be summarized as follows.

(1) The history of gas evolution and star formation in the solar neighborhood is not sensitive to the Gaussian and exponential infall rates. For the solar neighborhood, either a Gaussian or an exponential infall rate can well fit the observed G-dwarf metallicity distribution. The model predictions are also compatible with the observed [O/Fe] vs. [Fe/H] relation. If the infall time scale is kept constant, then the predicted behavior for the current properties of the Galactic disk is also similar for the Gaussian and exponential infall rates. The adoption of radial dependence of infall time scale will influence the disk evolution. It is difficult to judge which situation (varying or constant infall time scale) would be more realistic by the current available observations.

(2) The predicted current element abundance profile is not sensitive to details of the infall after the process of chemical enrichment reached a certain level. Concerning the time evolution of the gradient, we suggest that the so-called discrepancy of the gradient evolution among various models could not be described by only one word “steeper” or “flatter”. A single linear value of gradient strongly depends on how it is calculated. The situation could be different between the inner and outer disk. The gradient evolution is not only dependent on the adopted forms of the SFR and infall rate but is also significantly affected by the chemical composition of the infalling gas.

(3) Our new treatment of star formation law has resulted in a tighter dependence of SFR on gas surface density than that in Chang et al. (1999). This has a significant effect on the star formation and gas evolution of the whole disk.

**Acknowledgements** We thank the referee Helio Jaques Rocha-Pinto for his helpful comments and suggestions to improve this paper. This work was made possible thanks to the support of National Natural Sciences Foundation of China (No. 19873014) and the NKBRSF19990754.

## References

Allen C., Carigi L., Peimbert M., 1998, ApJ, 494, 247
Barbuy B., 1988, A&A, 191, 121
Berczik P., 1999, A&A, 348, 371
Blitz L., Spergel D. N., Teuben P., Hartmann D., Burton W. B., 1999, ApJ, 514, 818
Boissier S., Prantzos N., 1999, MNRAS, 307, 857
Carigi L., 1996, Rev. Mex. Astron. & Astrofis., 4, 123
Chamcham K., Tayler R. J., 1994, MNRAS, 266, 282
Chang R. X., Hou J. L., Shu C. G., Fu C. Q., 1999, A&A, 350, 38
Chiappini C., Matteucci F., Gratton R., 1997, ApJ, 477, 765
Chiappini C., Matteucci F., Romano D., 2001, ApJ, 554, 1044
Chen Y. Q., Nissen P. E., Zhao G., Zhang H. W., Benoni T., 2000, A&AS, 141, 491
Dame T. M., In: S. Holt, F. Verter (AIP), eds., Back to the Galaxy, p.267
Deharveng L., Pena M., Caplan J., Costero R., 2000, MNRAS, 311, 329
Edvardsson B., Andersen J., Gustafsson B. et al., 1993, A&A, 275, 101
Efstathiou G., 2000, MNRAS, 317, 697
Ferrini F., Mollá M., Pardi M. C., Diaz A., 1994, ApJ, 427, 745
Fich M., Silkey M., 1991, ApJ, 366, 107
Firmani C., Hernandez X., Gallagher J., 1996, A&A, 308, 403
Freeman K. C., 1970, ApJ, 160, 811
Giovagnoli A., Tosi M., 1995, MNRAS, 273, 499
Goswami A., Prantzos N., 2000, A&A, 359, 191
Götz M., Köppen J., 1992, A&A, 262, 455
Guibert J., Lequeux J., Viallefond F., 1978, A&A, 68, 1
Gummersbach C. A., Kaufer A., Schafer D. R. et al. 1998, A&A, 338, 881
Gusten R., Mezger M., 1983, Vistas Astr., 26, 159
Haywood M., 2001, MNRAS, 325, 1365
Hou J. L., Chang R. X., Fu C. Q., 1998, In: Kiwing Lam Chan, K. S. Cheng, H. P. Singh, eds., ASP Conf. Ser. Vol. 138, Pacific Rim Conference on Stellar Astrophysics, p.143
Hou J. L., Prantzos N., Boissier S., 2000, A&A, 362, 921
Israelian G., Garcia-Lopez R., Rebolo R., 1998, ApJ, 507, 805
Jog C. J., Solomon P. M., 1984, ApJ, 276, 114
Kauffmann G., White S. D. M., Guiderdoni B., 1993, MNRAS 263, 201
Kennicutt R. C. Jr., 1989, ApJ, 344, 685
Kennicutt R. C. Jr., 1998, ApJ, 498, 541
Kroupa P., Tout C., Gilmore G., 1993, MNRAS, 262, 545
Liang Y. C., Zhao G., Shi J. R., 2001, A&A, 374, 936
Lyne A., Manchester R., Taylor J., 1985, MNRAS, 213, 613
Maciel W. J., Quireza C., 1999, A&A, 345, 629
Matteucci F., Greggio L., 1986, A&A, 154, 279
Mo H. J., Mao S., White S. D. M., 1998, MNRAS, 304, 175
Mollá M., Ferrini F., Diaz A. I., 1997, ApJ, 475, 519
Navarro J. F., Frenk C. S., White S. D. M., 1996, ApJ, 462, 536
Pagel B. E. J., 1997, Nucleosynthesis and Galactic Chemical Evolution, Cambridge: Cambridge Univ. Press
Portinari L., Chiosi C., 1999, A&A, 350, 827
Portinari L., Chiosi C., 2000, A&A, 355, 929
Prantzos N., Aubert O., 1995, A&A, 302, 69

Prantzos N., Silk J., 1998, ApJ, 507, 229
Qian Y. Z., Wasserburg G. J., 2001, ApJ, 549, 337
Rana N. C., 1991, ARA&A, 29, 129
Robin A. C., Haywood M., Creze M. et al., 1996, A&A, 305, 125
Rocha-Pinto H. J., Maciel W. J., 1996, MNRAS, 279, 447
Rocha-Pinto H. J., Maciel W. J., Scalo J., Flynn C., 2000a, A&A, 358, 869
Rocha-Pinto H. J., Maciel W. J., Scalo J., Flynn C., 2000b, A&A, 358, 850
Sackett P. D., 1997, ApJ, 483, 103
Samland M., Hensler G., Theis C. H., 1997, ApJ, 476, 544
Scalo J., 1986, Fund. Cosmic Physics, 11, 1
Scoville N., Sanders D., 1987, In: H. Thronson, D. Hollenbach eds., Interstellar Processes, Kluwer, p.21
Shaver P. A., McGee R. X., Newton L. M. et al., 1983, MNRAS, 204, 53
Simpson J. P., Colgan S. W. J., Rubin R. H., Erickson E. F., Haas M. R., 1995, ApJ, 444, 721
Smartt S. J., Rolleston W. R. J., 1997, ApJ, 481, L47
Smartt S. J., Venn K. A., Dufton P. L. et al., 2001, A&A, 367, 86
Somerville R. S., Primack J. R., 1999, MNRAS, 310, 1087
Steinmetz M., Müller E., 1994, A&A, 281, L97
Thon R., Meusinger H., 1998, A&A, 338, 413
Tosi M., 1988, A&A, 197, 47
Tsujimoto T., Yoshii Y., Nomoto K., Shigeyama T., 1995, A&A, 302, 704
Twarog B. A., Ashman K. A., Anthony-Twarog B. J., 1997, AJ, 114, 2556
Vilchez J. M., Esteban C., 1996, MNRAS, 280, 720
Wakker B. P., Howk J. C., Savage B. D. et al., 1999, Nature, 402, 388
White S. D. M., Frenck C. S., 1991, ApJ, 498, 541
White S. D. M., Rees M. J., 1978, MNRAS, 183, 341
Woosley S. E., Weaver T. A., 1995, ApJS, 101, 181
Woosley S. E., 1997, ApJ, 476, 801